INTERNATIONAL ATOMIC ENERGY AGENCY
UNITED NATIONS EDUCATIONAL, SCIENTIFIC AND CULTURAL ORGANIZATION
INTERNATIONAL CENTRE FOR THEORETICAL PHYSICS
I.C.T.P., P.O. BOX 586, 34100 TRIESTE, ITALY. CABLE: CENTRATOM TRIESTE

SMR.380/16

COLLEGE ON THEORETICAL AND EXPERIMENTAL RADIOPROPAGATION SCIENCE

6 - 24 February 1989

LECTURES 5 & 6: SOME ASPECTS OF RADIOWAVE PROPAGATION IN THE TROPOSPHERE

G.O. AJAYI

Department of Electronic and Electrical Engineering
Obafemi Awolowo University
Ile-Ife, Nigeria

TABLE OF CONTENTS

1. TERRESTRIAL LINE OF SIGHT SYSTEMS.

Some propagation problems to be taken into consideration are:

(i) diffraction fading due to obstruction of the path by terrain obstacles under adverse conditions of refractive index variation with height.

(ii) fading due to
  (a) atmospheric multipath or defocussing associated with abnormal refractive layers.
  (b) multipath from surface reflection

(iii) attenuation due to
  (a) rain, other hydrometeors and solid particles in the atmosphere
  (b) atmospheric gases.

(iv) reduction in cross-polarization discrimination due to
  (a) multipath
  (b) Precipitation.

(v) variation of the angle of arrival at the receiver terminal and angle-of-launch at the transmitter terminal due to refraction.

(vi) Signal distortion due to
  (a) frequency selective fading
  (b) delay during multipath propagation.

1.1 Path Profile

An important factor when plotting a profile chart is the relative curvature of the earth and the microwave beam. This is taken care of by the effective earth radius factor, k. This relative curvature can be shown graphically either as a curved earth with radius KR and a straight line beam, or as a flat earth with a microwave beam having a curvature of KR. The latter method is preferred because

(i) it permits investigation of the conditions for several values of K to be made on one chart.

(ii) eliminates the need for special earth curvature graph paper.

(iii) facilitates the task of profile plotting.

A typical path profile is shown in Fig. 1.

1.2 Terrain Effects

Terrain has two effects on the propagation loss.

(i) Trees, buildings, hills or the earth can block a portion of the microwave beam to cause an obstruction loss.

(ii) a very smooth section of terrain or water can reflect a second signal to the receiving antenna leading to loss and variation of received signal.

(a) Obstruction

This is a form of diffraction loss. The loss increases with decreasing path clearance from zero loss (i.e. free space conditions) to about 10dB for zero clearance. For negative clearance (i.e. obstructed path) the obstruction loss increases very rapidly until the path is no longer usable. Fig. 2 shows the obstruction loss versus path clearance in terms of Fresnel zones. [Lenkurt, 1962]

The n^{th} Fresnel zone radius is given by

$$F_n = \left(n\lambda d_1 d_2 / d\right)^{1/2} \quad ---(1)$$

where d_1 and d_2 are distances from the ends of the link and d is length of link.

Fig. 2 shows that the obstruction loss is zero for a path clearance of approximately $0.6F_1$; where F_1 is the first Fresnel zone radius.

$$F_1 = 17.3\sqrt{\frac{d_1 d_2}{f d}} \quad ---(2)$$

where f is frequency (GHz), and d_1, d_2, d in km.

The diffraction loss over average terrain can be approximated for losses greater than about 15dB by (CCIR, 1982) - based on U.S.A. measurements.

$$A_d = -20h/F_1 + 10 \text{ dB} \quad ---(3)$$

where h/F_1 is the normalized path clearance

Fig. 3 shows the CCIR recommendations for diffraction loss.

The reflection coefficient R in fig. 2 is a function of the smoothness of the terrain. R = 0 for knife-edge diffraction and R = -1

for smooth sphere diffraction. Due to large obstruction losses encountered when the path clearance is less than zero, microwave paths are usually planned so that even during adverse atmospheric conditions the clearance is zero or better.

(b) Reflection

When there is more than $0.6F_1$ clearance, the received signal can be less or greater than the free space value depending on the relative strength and phase of the reflected signal. The direct and reflected waves interfere and result in maxima and minima patterns, called the "Fresnel pattern" as the clearance is increased above grazing. This can be observed in fig. 2. The maxima and minima alternate with the odd and even numbered zones as the clearance is increased.

Microwave paths with highly reflective terrain are undesirable and should be avoided when possible. Changes in N profile slope (hence Ic) will cause the point of reflection to shift by changing the amount of path clearance. This leads to variations in the received signal strength. Some of the techniques used to eliminate strong reflections from water, salt flats and other smooth terrain are

(i) a different route could be selected

(ii) sites could be selected so that screening can be obtained from foreground terrain, at either or both ends of the path, to [illegible] reflected ray.

(iii) Antenna heights could be adjusted to prevent reflection from smooth terrain or water. Nomograms exist for determination of the reflection point.

1.3 Planning criteria for path clearance

The following procedure is recommended by CCIR, 1988

(i) determine the antenna heights required for the appropriate median value of the point k-factor (in the absence of any data, use $k = 4/3$ and $1.0F_1$ clearance over the highest obstacle (temperate and tropical climates).

(ii) obtain the value of K_e (99.9%) from fig. 4 for the path considered.

(iii) calculate the antenna heights required for the value of K_e obtained from step (ii) and the following Fresnel zone clearance radii.

Temperate climate

$0.0F_1$ (ie grazing) if there is a single isolated path obstruction

$0.3F_1$ if the path obstruction is extended along a portion of the path

Tropical climate

$0.6F_1$ for path length greater than about 30km.

(iv) use the larger of the antenna heights obtained by steps (i) and (iii).

1.4 Angles of arrival

The variation of the angle of arrival in the vertical plane is approximately proportional to the path length. The variations are caused by changes in the mean refractive

index gradient. Deviations from the normal angle of arrival vary widely under multipath conditions and do not exhibit a strong dependence on path length.

1.5 Free space path attenuation:

The basic free space transmission loss, L_b is the ratio of the radio frequency power radiated in free space from an ideal loss-free isotropic ($G = 1$) transmitting antenna to the power available from an ideal loss free isotropic receiving antenna.

The power flux per unit area, P_a at a distance d (m) from a transmitter radiating a power P_t (W) from an isotropic loss-free antenna is given by

$$P_a = P_t / 4\pi d^2 \quad \text{---} \quad (4)$$

The received power is $P_a \cdot A_e$, where A_e is effective aperture given by

$$A_e = G\frac{\lambda^2}{4\pi} \quad \text{---} \quad (5)$$

$$L_b = P_t/P_r = (4\pi d/\lambda)^2 \quad \text{---} \quad (6)$$

where P_r is the received power and d and λ are in the same units.

$$L_b = 92.44 + 20\log d + 20\log f \quad \text{---} \quad (7)$$

where d is in km and f in GHz

or $$L_b = 32.44 + 20\log d + 20\log f \quad \text{---} \quad (8)$$

where d is in km and f in MHz

Figure 5 shows the variation of the free space path loss.

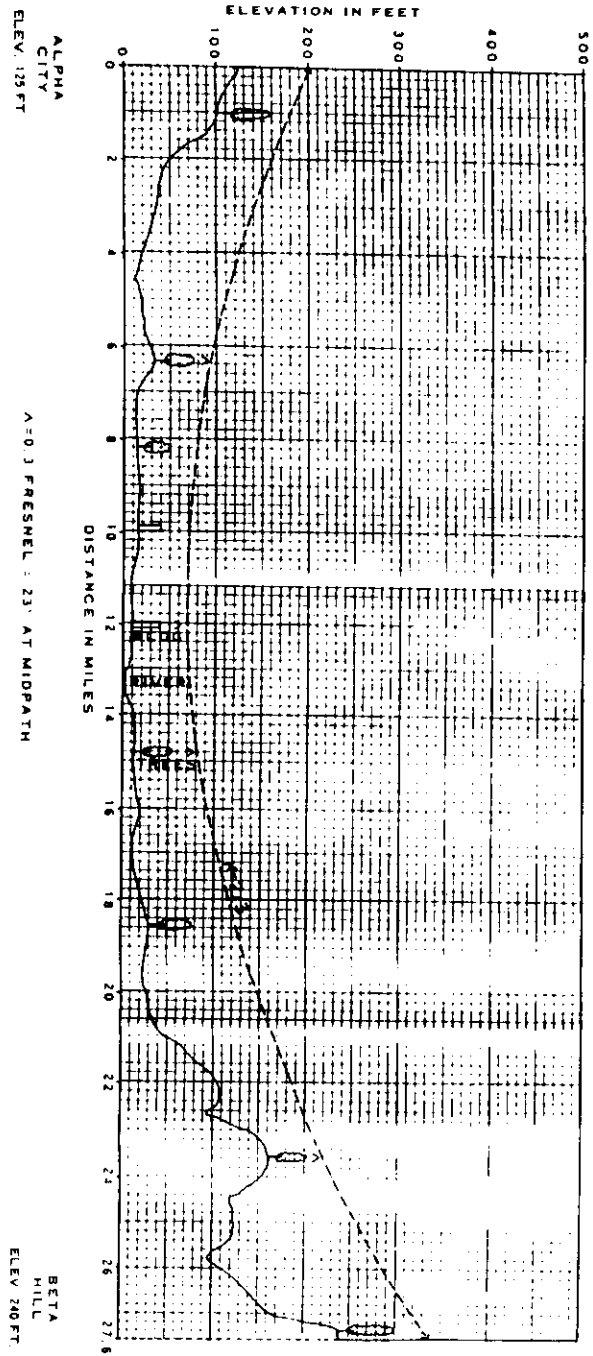

Fig. 1: Typical Topographic Profile (After Lenkurt, 1960)

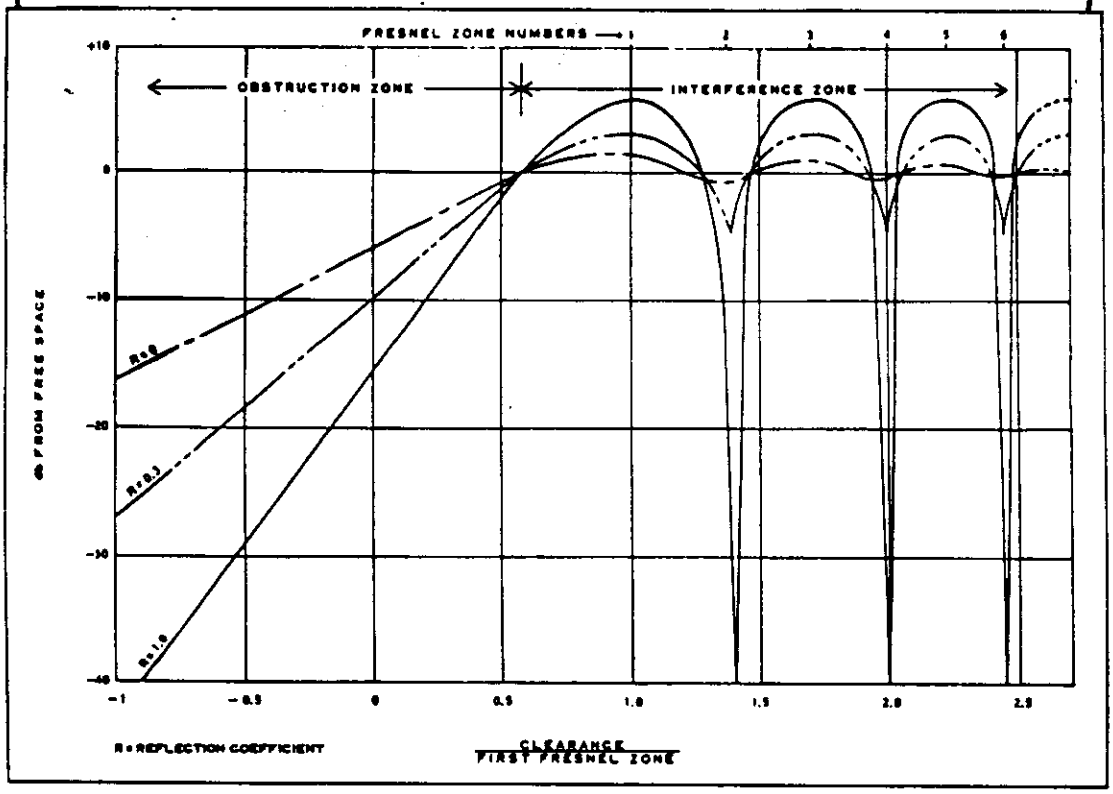

FIGURE 2
Attenuation vs. Path Clearance [Lenkurt].

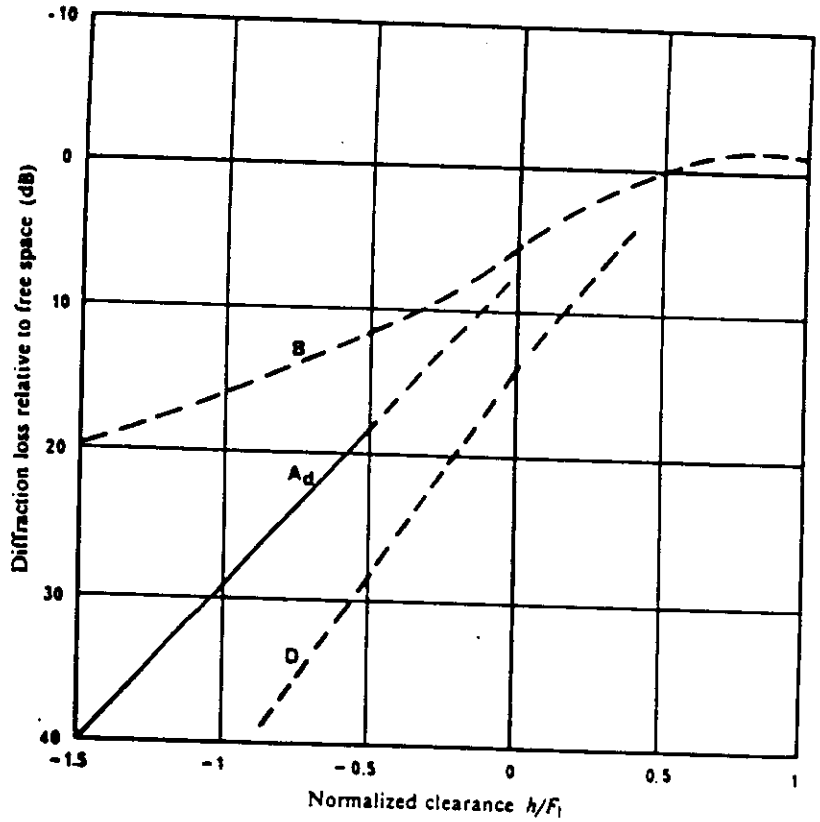

FIGURE 3 – *Diffraction loss for obstructed line-of-sight microwave radio paths* [CCIR]

B : the theoretical knife-edge loss curve,
D : the theoretical smooth spherical Earth loss curve,
A_d : an empirical diffraction loss derived in the United States for intermediate terrain,
h : the amount by which the radio path clears the Earth's surface and
F_1 : the radius of the first Fresnel zone

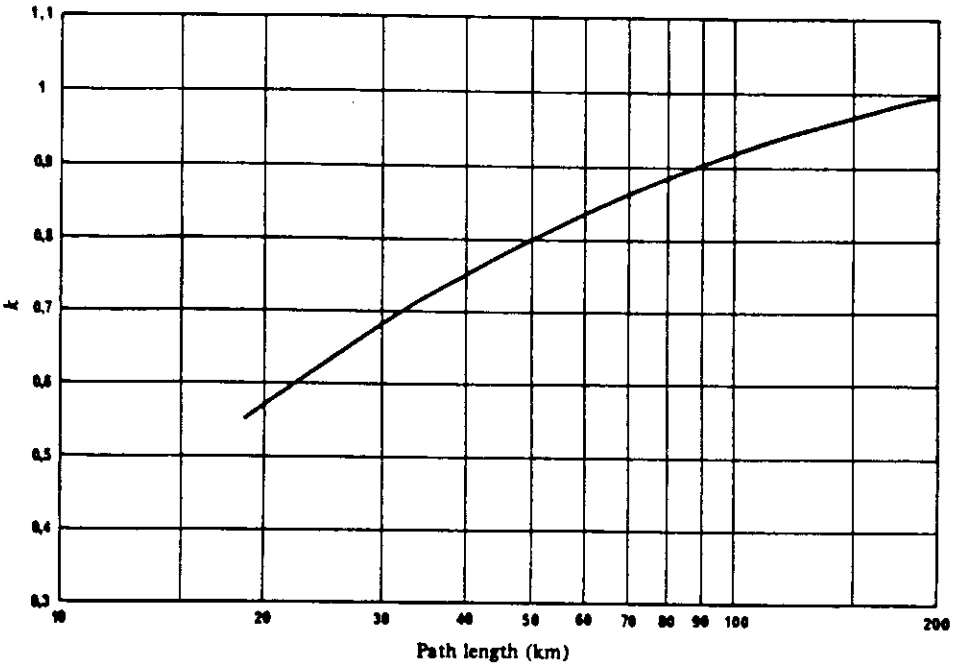

FIGURE 4 — *Minimum effective value of k exceeded for approximately 99.9% of the time (Continental temperate climate)* [CCIR, 1982]

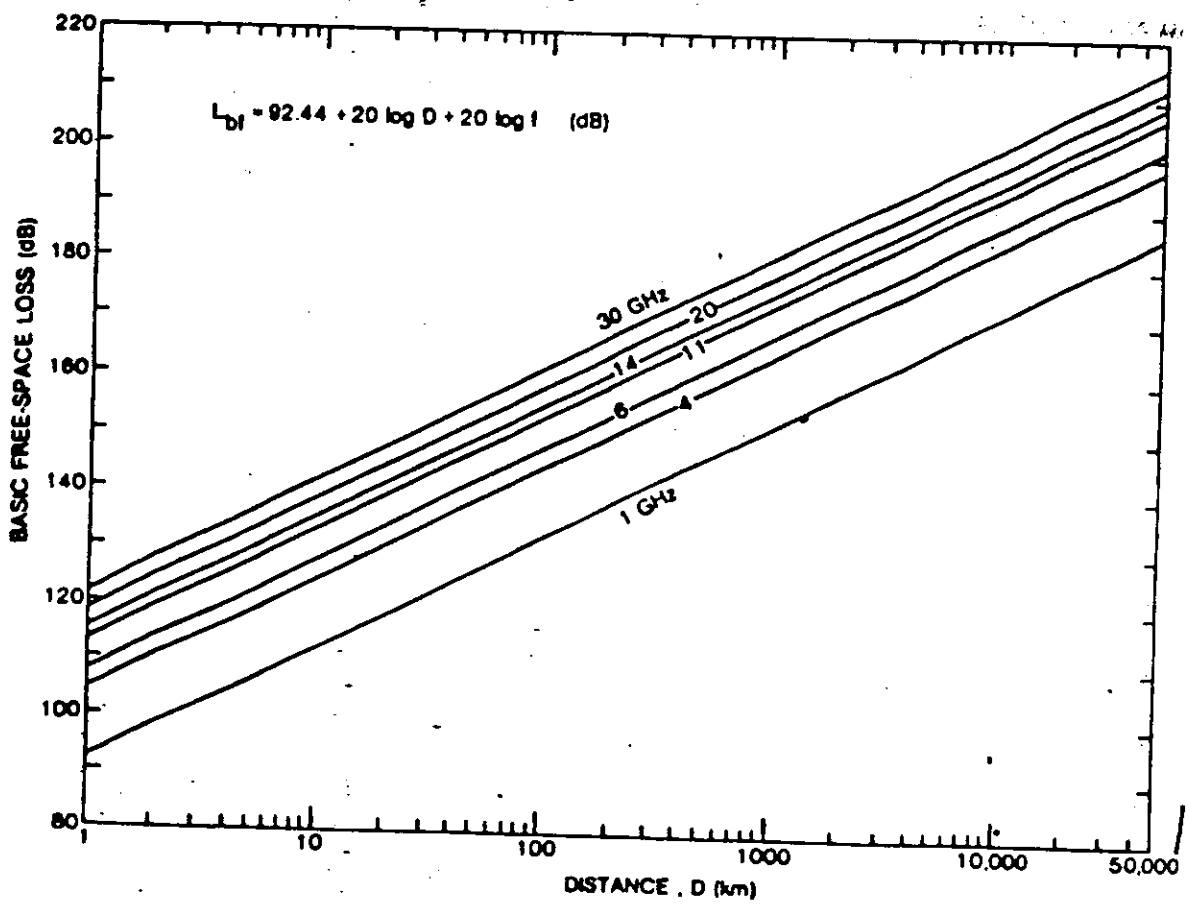

Figure 5 : Free space path Loss.

1.6 Multipath Propagation

The presence of distinct propagation paths give rise to variations in the received signal (amplitude and phase) in accordance with the mutual relationship between the amplitudes and phases of the separate signal contributions. The main effect is the generation of fades, which includes variations of the amplitude, the phase, and the polarization of the received signal. Multipath fading (MPF) is a principal cause of outage in medium and high capacity microwave digital radio systems.

1.6.1 Multipath parameters and distribution functions

The transfer function, $H(f)$ representing the deviations from the normal propagation transfer function is given by

$$H(f) = \sum_{n=1}^{N} a_n \exp(-j2\pi f \tau_n) \quad ----- (9)$$

where N = number of propagation paths
a_n, and τ_n are amplitude and delay (the propagation time) for each separate path,
f is frequency.

If a signal is composed of a large number of independent components with uniformly distributed phases and with no predominant term, the resultant phase distribution will be uniform and the amplitude, R will be Rayleigh distributed.

$$P(R \leq r) = 1 - e^{-\frac{r^2}{\Omega}} \quad -- (10)$$

where Ω = mean-square value of R.

If the signal consists of a constant signal (e.g. direct signal) plus a random signal contribution where the random term is Rayleigh distributed, then the amplitude probability function is described by an expression involving integrals of a modified Bessel-function. This distribution is known as the Rice-Nakagami distribution or an n-distribution. The phase distribution is non-uniform. [Stephansen, 1982].

The diurnal and seasonal variations of multipath propagation are closely related to the occurrence of the meteorological conditions causing multipath propagation.

The statistical distribution of signals received under multipath propagation can be separated into a statistical distribution function characterizing the propagation phenomena, and a probability of occurrence of the phenomena. A general function for estimating the probability of fading is given by [Stephansen, 1

$$P(R \leq L) = K \cdot Q \cdot f^{B} \cdot d^{C} F_n^{\alpha} L^{2} \quad --- (11)$$

where P is the probability.
R and L are amplitudes in linear measure.
K is a factor for climatic conditions
Q is a factor for terrain conditions
f is the frequency (GHz)
d is the path length in km.
f_n is a path clearance factor
B, C and α are constants.

1.6.2: Fading due to multipath and related mechanisms

Paths with strong surface reflections are not considered because it is advisable to avoid such paths. The fading can be divided into 3 types:

(i) rapid scintillation – not significant. More noticeable at frequencies above 10 GHz – these are usually small amplitude fluctuations

(ii) slow non-selective fading due to single path propagation effects. It occurs during stratified atmospheric conditions. Less severe than multipath fading. It has been attributed to

(a) atmospheric beam defocusing, which can persist for hours and is common over water and coastal areas. Olsen et al, 1987 suggests that the fading is caused by layers of large negative refractivity gradients situated below the path.

(b) antenna beam decoupling caused by large angle-of-arrival variations, which can be significant on long paths if the antenna beamwidths are very narrow.

(iii) rapid frequency-selective fading due to multipath propagation. It is the most severe and governs the outage of analogue and digital radio links. Because the fading is frequency selective, the distortion induced at all amplitude levels in a wideband digital link can be a major source of outage. Multipath propagation reduces the cross-polarization isolation in a dual-polarized link.

Conditions for fade types (ii) and (iii) occur during the night and early morning hours of Summer days in the temperate ~~reg~~ climates. In the tropics (especially at the coastal locations) the fades have a higher incidence of occurrence.

1.7 Diversity Improvement

Diversity system is used to reduce signal fading by selecting the highest level from two or more signal channels which carry the same information, but are taken from separate receivers, so long as the signals have a low cross-correlation.

Frequency diversity — different frequencies

Space diversity — two receiving channels are fed from two antennas spaced a distance apart.

Quadruple-channel diversity — use of both frequency and space diversities

Angle Diversity — use of two or more antenna beams separated by small angles in the vertical plane

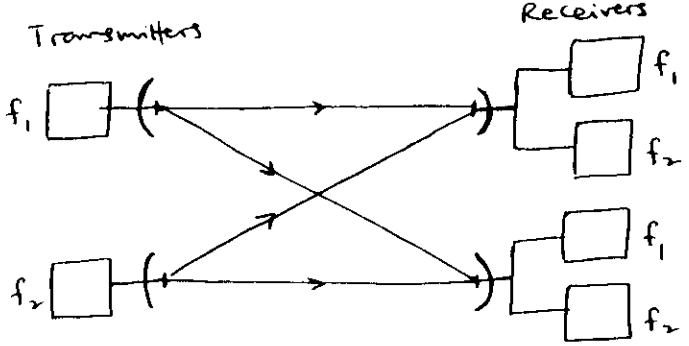

fig. 6 Quadruple diversity system

The diversity improvement factor, I is given by

$$I = \frac{P_r(W)}{P_{rd}(W)} \quad \text{---} \quad (12)$$

where $P_r(W)$ is the probability for the unprotected path, $P_{rd}(W)$ the probability that diversity paths will receive a power less than W simultaneously.

1.7.1 Space-diversity

Vertical spacing of 150λ is desirable for space diversity to be effective.

In areas where ducting is prevalent e.g. in Senegal and parts of West Africa (Hontefeuille et al. 198?) measurements indicate that diversity using parallel radio paths properly spaced above the ground could lead to significant improvement in reception.

A widely used (CCIR, 1988) prediction equation is given by

$$I = S^2 (f/d)\, 10^{(A-V)/10} \cdot 1.2 \times 10^{-3} \quad \text{---} \quad (13)$$

where
A = fade depth (dB)
S = vertical separation of receiving antennas (m), centre to centre ($5 \le S \le 15$)
f = frequency (GHz) ($2 \le f \le 11$)
d = path length (km) ($24 \le d \le 70$)
and $V = |G_1 - G_2|$ where G_1 and G_2 are the gains of the two antennas.

The equation is valid only for $I \ge 10$.

for $d > 75$ km, the Rayleigh-type fading may no longer be applicable and I is given (CCIR, 1988)

$$I = 1 + 1.14 \times 10^{-7} (S \cdot f)^{1.2} \cdot d^{1.5} / P_r(W) \quad \text{---} \quad (14)$$

for $2.1 < f < 6.2$ GHz, $50 < d < 240$ km, $63 < S/\lambda < 270$ where λ is wavelength (m).

1.7.2 Frequency-diversity factor

The frequency-diversity improvement factor can be estimated (CCIR, 1988) from

$$I = \frac{0.8}{f \cdot d} \left(\frac{\Delta f}{f}\right) \cdot 10^{A/10} \quad \text{---} \quad (15)$$

where f = band centre frequency (GHz)
d = path length (km); A = fade depth
$\Delta f/f$ = relative frequency spacing as a percentage.

applicable when

$2 \le f \le 11$ GHz
$30 \le d \le 70$ km
$\Delta f/f \le 5\%$

figure 7 (Dougherty & Dutton, 1981) shows an example of an atmospheric fading mechanism.

figure 8 shows the variation of frequency-diversity improvement factor, I, (CCIR, 1982).

1.7.3 Systems consideration

In analogue FM-FDM systems multipath transmission contributes to an increase in the thermal noise (due to power fading) and in the intermodulation noise (due to frequency selectivity). The thermal noise variation due to multipath fading is accumulated at the circuit end. Although it has been shown (Stephansen, 1960) that intermodulation noise is insignificant compared to the thermal noise for bandwidths up to (at least) 12 MHz and path lengths of up to about 100 km, there are indications that on very long paths, the intermodulation noise may be of importance.

In digital radio systems, the multipath propagation contributes to thermal noise and inter symbol interference. Inter symbol interference gives the major system impairment. The effect of multipath propagation on digital radio systems depends on the digital signal format, such as the bandwidth, the number of levels and the modulation method. In many digital systems an amplitude dispersion of 5dB will give unacceptable high bit-error-rates.

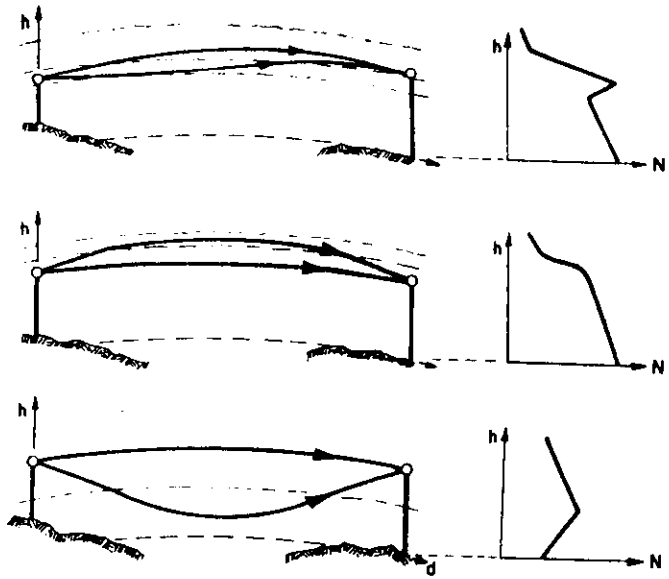

Figure 7: An atmospheric fading mechanism, Multipath
[Dougherty and Dutton, 1981]

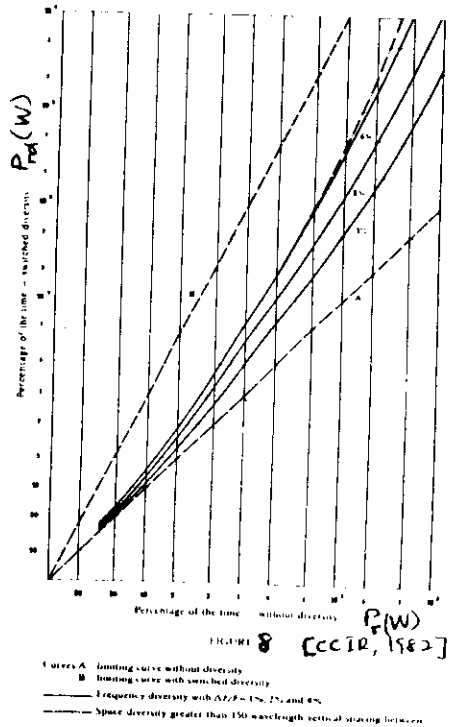

FIGURE 8 [CCIR, 1982]

1.8 Path Attenuation due to precipitation

The following simple technique is recommended by the CCIR, 1986 for the estimation of the long-term rain attenuation statistics.

(i) Obtain $R_{0.01}$ i.e. the rain rate exceeded for 0.01% of time with an integration time of 1 minute. If local value is unavailable, the CCIR value can be utilized.

(ii) Obtain the specific attenuation for the frequency, polarization and rain rate of interest.

(iii) Obtain effective path length, L_{eff} from the relation $L_{eff} = rL$

where r = reduction factor and L the physical length of the path.

$$r = \frac{1}{1 + 0.045L} \quad \text{---(16)}$$

(iv) Path attenuation $A_{0.01}$ exceeded for 0.01% of time is given by

$$A_{0.01} = \gamma L_{eff} = \gamma L r \quad \text{---(17)}$$

where γ = specific attenuation at the rain rate obtained in (i).

(v) for percentages of time, p between 0.001 and 1.0, the following power law can be used

$$\frac{A_p}{A_{0.01}} = 0.12\, p^{-(0.546 + 0.043 \log p)} \quad \text{---(18)}$$

The factors are 0.12, 0.39, 1 and 2.14 for 1%, 0.1%, [illegible] and 0.001% respectively.

(vi) $$p = 0.3\, P_w^{1.15} \quad \text{---(19)}$$

where p is the average annual probability of exceeding a given attenuation level and P_w is the worst-month probability

The steps outlined above were based on results obtained in Europe, Japan and U.S.A. for simultaneous rain rate and attenuation measurements, mean error is about -5% and standard deviation between 10 and 15% as a function of percentage of time.

The above technique is based on the use of the effective radio path length to account for the horizontal inhomogeneity of rainfall along the path. The concept of path averaged rain rate has also been employed, where

$$r = \frac{\bar{R}}{R_p} \quad \text{---(20)}$$

where $\bar{R}$ is path averaged rain rate and R_p is the surface rain rate.

Crane, 1989 has shown that a power law exists between r and R_p.

Making use the effective path length technique, Manpforuma, 1987 have proposed the following prediction technique, which is applicable to more climatic zones. A correction coefficient, C has been used instead of the reduction factor, r.

$$A(L, f, R_p, P) = \gamma(R_p) \cdot C(L, f, R_p, P) \cdot L \quad \text{--}$$

where the correction coefficient is given by

$$C(L, f, R_p, P) = \frac{U(P)(R_{0.01}/R_p)^{V(L)}}{1 + \eta (P/0.01)^{-0.36} L^{m(f,L)}} \quad \text{---(22)}$$

where $R_{0.01}$ and R_p represent point rainfall rates observed on the radio path during 0.01% and P(%) of the time, respectively, P being the same time percentage for which the attenuation exceedance is to be calculated.

$$m(f, L) = 1 + 1.4\, 10^{-4} f^{1.76} \log_e(L) \quad \text{- - - -(23)}$$

where f is frequency in GHz and P(%) the time percentage for which the rain attenuation is predicted.

The frequency dependence of C is due to both the inhomogeneity of rain along the path and to the non-linearity of the relationship between specific attenuation and rain rate.

U depends on type of path - terrestrial or earth-satellite. for any path, U and η are given by

$$V(L) = 0.38\, L^{-0.25} \quad \text{- - - (24)}$$

$$\eta = \begin{cases} 0 & \text{if } L < 5 \text{ km and } f < 25 \text{ GHz} \\ 0.03 & \text{in all other cases} \end{cases} \quad \text{- - - (25)}$$

Moupfouma (1987) also showed that for f < 25GHz, the rain effects observed on a radio link with a path length less than 5 km, are similar to those due to a uniform rainfall on the whole path considered.

Values of parameter U for terrestrial links are shown in Table 1. Figure 9 shows the behavior of the correction coefficient for terrestrial paths.

1.9 Polarization Scaling

$$A_V = \frac{300\, A_H}{335 + A_H} \quad \text{- - - - (26)}$$

$$A_H = \frac{335\, A_V}{300 - A_V} \quad \text{- - - - (27)}$$

The equations are useful when long term attenuation statistics exist at one polarization and the attenuation over the same link is to be estimated for another polarization.

H, V refer to horizontal and vertical polarizations

Characteristics of the radio path	Expressions of U(P) as function of P	
	$P \le 0.01\%$	$P > 0.01\%$
$L < 5$ km and $f < 25$GHz	$821.4P^2 - 34.6 + 1.3$	$0.93\, e^{4.14P}$
$L \ge 50$km with any f	$0.74\, P^{-0.07}$	$1.48\, P^{0.105}$
All other cases	$0.71\, P^{-0.07}$	$0.89\, e^{1.6P}$

Table 1: Values of U for terrestrial links (Moupfouma, 1987)

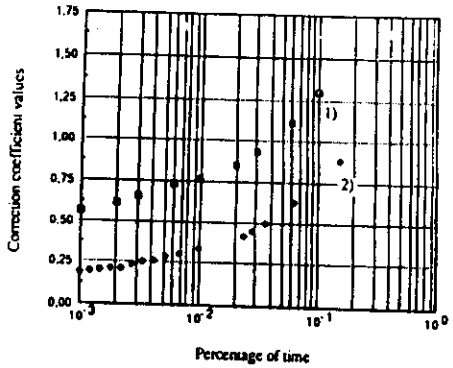

FIG. 9 — Behaviour of the correction coefficient for terrestrial paths.
1) Mendlesham - UK (7.4 km, 19.4 GHz - V).
2) Paris - France (58 km, 11.7 GHz - H).

[After Manpfouma, 1987]

2. EARTH - SATELLITE PATH

2.1 Attenuation due to precipitation and Clouds.

2.1.1 Vertical structure of precipitation

A vertically homogeneous and cylindrical model of a raincell extending from the earth's surface up to the 0°C isotherm height has been assumed in prediction models for attenuation. The simple raincell model has given good results for the temperate latitude. The model overestimates the attenuation in the tropical regions because of the heavy rainfall, the different character of tropical rain with different horizontal and vertical structure and/or different drop size distribution.

Below the 0°C isotherm, we have only liquid particles that attenuate the signals.

Above the 0°C isotherm, we have only freezing particles with negligible attenuation on the radio waves.

The average height of the 0°C isotherm h_{FR} during rainy conditions is given by (CCIR, 1988) as

$$h_{FR}(km) = \begin{cases} 4.0 & \text{for } 0 < \phi < 36° \\ 4.0 - 0.075(\phi - 36) & \text{for } \phi \geq 36° \end{cases} \quad \text{---- (28)}$$

where ϕ is the latitude (degrees).

There is little data base for the tropics in order to confirm if the above values will be adequate. However, Ajayi and Odumeru, 1989

showed that the value obtained in Nigeria is generally higher than the CCIR values.

The effective rain height, h_R for prediction of attenuation is in general different from the 0°C isotherm height for Europe

$$h_R \approx h_{FR}$$

Rue, 1988 have proposed a rain height model which is dependent on the 0.01% rain rate.

$$h_R = \begin{cases} h_L + \dfrac{h_{FR} - h_L}{R_{FR} - R_L}(R - R_L) & R_{FR} < R < R_L \;;\; h_{FR} > h_L \\ h_L & R \geq R_L \\ h_{FR} & R \leq R_{FR} \\ h_{FR} & h_{FR} \leq h_L \end{cases} \quad \text{---(29)}$$

where

R = the rain intensity, $R_{0.01}$

$R_L = 70$ mm/h

$R_{FR} = 50$ mm/h

$h_L = 2.8$ km

h_{FR} = 0°C isotherm height during raining conditions

This model is currently being considered by CCIR for adoption.

2.1.2 Average year attenuation prediction

Parameters required are:

$R_{0.01}$: point rainfall rate at the location for 0.01% of an average year (mm/h)

h_s : height above mean sea level of the earth station (km)

θ : elevation angle

ϕ : latitude of earth station (degrees)

f : frequency (GHz)

To predict slant path attenuation exceeded for 0.01% of the time, we have the following steps:

(i) Assuming $h_R \approx h_{FR}$. Use equation (28) (Note that it may not be valid at low latitudes).

(ii) For $\theta \geq 5°$, the slant path below the rain height is given by

$$L_s = \frac{(h_R - h_s)}{\sin\theta} \text{ km.} \quad \text{---(30)}$$

for $\theta < 5^\circ$

$$L_s = \frac{2(h_R - h_s)}{\left(\sin^2\theta + \frac{2(h_R - h_s)}{Re}\right)^{1/2} + \sin\theta} \quad \text{km.} \quad \text{---(31)}$$

(iii) Horizontal projection, L_G of the slant path is given by (Refer to Fig. 10)

$$L_G = L_s \cos\theta \quad \text{----(32)}$$

(iv) The reduction factor, $r_{0.01}$ for 0.01 % of the time is given by

$$r_{0.01} = \frac{1}{1 + 0.045 L_G} \quad \text{---(33)}$$

(v) Local value of $R_{0.01}$, rain rate exceeded for 0.01 % of time, for an integration time of 1 minute. If local $R_{0.01}$ is unavailable, value from CCIR climatic zone map is used.

(vi) Specific attenuation γ_R is given by

$$\gamma_R = a (R_{0.01})^b \quad \text{---(34)}$$

Use frequency dependent values of a and b.

(vii) The attenuation exceeded for 0.01 % of an average year is given by

$$A_{0.01} = \gamma_R \cdot L_s \cdot r_{0.01} \quad (dB) \quad \text{--(35)}$$

For other percentages of an average year, the attenuation, A_p exceeded is given by

$$\frac{A_p}{A_{0.01}} = 0.12\, P^{-(0.546 + 0.043 \log P)} \quad \text{---(36}$$

The factors are 0.12, 0.38, 1 and 2.14 for 1 %, 0.1 %, 0.01 % and 0.001 % respectively.

For latitudes, $\phi > 30^\circ$, the prediction is in agreement within 10 % of measurements at 0.01 % level. For low latitudes the prediction overestimates and the predicted value is to be divided by 3 in order to obtain values comparable with available measurement data.

In order to extend the Manpfourma's prediction model to the slant path case, the $U(P)$ is given as in Table 2

Regions	Parameter U for slant paths as a function of time percentage P	
	$L_s \geq 5$ km	$L_s \leq 5$ km
Australia	$U = 0.24\, P^{-0.13}$	$U = 0.47 P^{0.02}$
Europe	$U = 1.11\, P^{-0.035}$	$U = -38P^2 + 7P + 0.65$
Japan	$U = 1.54P^2 - 1.3P + 0.9$	$U = 1.73 P^{0.12}$
USA	$U = -0.3P^2 - 0.007P + 0.82$	$U = 1.3 P^{0.06}$

Table 2 : Evaluation of parameter U for slant paths (Manpfourma 1987).

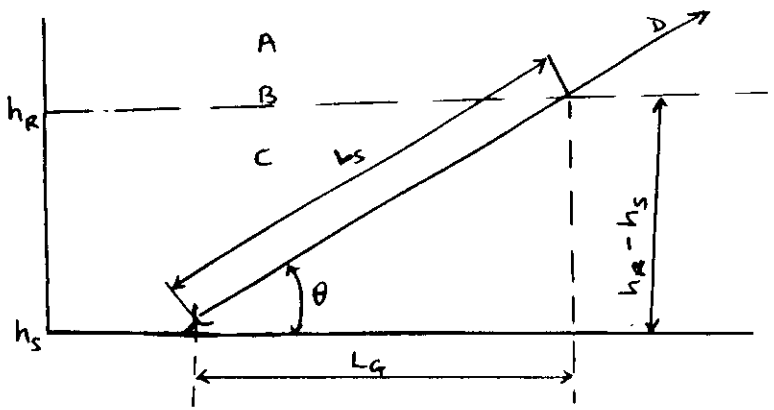

Figure 10 Schematic representation of an earth-space path.

A : Frozen precipitation
B : Rain height
C : Liquid precipitation
D : Earth - space path.

Note: The attenuation due to atmospheric gases on the earth - satellite path has been discussed earlier.

2.1.3 Site Diversity

Intense rain cells responsible for large attenuation usually have horizontal dimensions of a few km; hence site diversity is employed to improve system reliability.
Orbital diversity can also be considered for the improvement of system reliability.

3. TRANSHORIZON PROPAGATION

Can be broadly divided into two parts.

(i) Provision of radio relay systems
(ii) Interference to other systems.

3.1 Provision of radio relay systems.

for frequencies greater than 30 MHz, beyond the horizon propagation which occur permanently are due to

(a) diffraction – attenuation increases rapidly with distance, hence not suitable.
(b) scatter from atmospheric irregularities – used to establish transhorizon radio communication.

Practical frequency range: about 200 MHz – 5 GHz
distance – up to 1000 km.

Such systems require high power transmitters, high gain antennas, sensitive receivers and usually some diversity system to overcome signal fading.

3.1.1 Long term median transmission loss

The long term median transmission loss, L(50) due to tropospheric scatter has the form (CCIR, 1982)

$$L(50) = 30\log f - 20\log d + F(\theta d) - G_t - G_r + L_c - V(d_c) \quad \text{in dB} \quad (59)$$

where f is frequency (MHz), G_t, G_r are antenna gains, L_c is the aperture-to-medium coupling loss (or gain degradation) of the two antennas, θ (radians) is the angle between the radio horizons in the

great circle plane containing the path terminals for median atmospheric conditions, $F(\theta d)$ is a function of the angle θ (radians) and the distance d (km), shown in fig. 11 as a function of the surface refractivity, N_s. $V(de)$ is a correction for various types of climates (CCIR, 1982).

A semi-empirical estimate of L_c is given by

$$L_c = 0.07 \exp[0.055 (G_t + G_r)] \quad dB \quad ---(38)$$

$G_t < 50dB$, $G_r < 50dB$

In terms of the radio meteorological parameters, the basic transmission loss $L_b(P)$ for the time percentage P, in dB can be obtained from the semi-empirical formula

$$L_b(P) = 102 + 30 \log d + 30 \log f + 1.5 G_c \quad ---(39)$$

where
d = distance (km)
f = frequency (MHz)
G_c = index gradient near the base of the common volume (which can often be replaced by the difference between the value of N at 1km above and at the base of the common volume

3.1.2 Signal Variations

Two types: Slow and rapid signal variations.

(a) Slow variations are due to major changes in refractive index and is weather dependent. They are not strongly dependent on frequency. They may have cyclic periods of several hours, one or more days or seasons. Diurnal variations tend to produce maximum transmission loss in the afternoon, particularly during the summer, and on relatively short paths (100 – 150 km). At great distances e.g. 600 km the diurnal cycle can be such as to have maximum values during the day (Hall, 1979).

(b) Rapid fading

Typical frequencies are:
At VHF – a few fades per minute
At UHF – 0.1 to 1 Hz
At SHF – a few Hz

This is as a result of the vector addition of many incoherent contributions (i.e. with different amplitude and phase) from a large number of scattering elements within the common volume of the two antennas of the radio link. Analysis over periods of up to 5 min. shows that the amplitude distribution follows a Rayleigh law with $\sigma = 0$ (standard deviation).

The rapidly varying fading patter determines
(i) the transmissible bandwidth
(ii) the associated limitations to rate of transmission of digital data.
(iii) the gain degradation of the antennas that may be expected.

3.1.3 Diversity Systems

Effects associated with rapid fading can be overcome to some extent by diversity operation. Quadruple diversity (space and frequency) is widely used to achieve operational reliability of about 99.9%.

Adequate diversity spacings in the horizontal, Δ_h(m) and vertical Δ_v(m) for frequencies greater than 1 GHz is given by (CCIR, 1982) as

$$\Delta_h = 0.36\left(D^2 + 160\right)^{1/2} \quad - - - (40a)$$

and $$\Delta_v = 0.36\left(D^2 + 225\right)^{1/2} \quad - - - (40b)$$

The separation for frequency diversity for f > 1 GHz is given by

$$\Delta_f = \left(1.44 f/\theta d\right)\left(D^2 + 225\right)^{1/2} \quad - - - (41)$$

where D is antenna diameter (m), f (MHz) is frequency, θ (mrad) is the angle of scattering in the centre of the common volume, and d (km) is the path length.

Table 3 shows typical values.

d (km)	$\Delta f/f$ (%)	Δ (m)
≤ 200	3	200λ
> 200	1	100λ

Table 3 : Typical values of separation (space and frequency) for diversity systems.

Frequency/angle diversity can be employed. Only one antenna is used at each end of the link, but two vertically spaced feeds to the receiver

The technique is useful where large antennas and high land costs are involved or on offshore oil rig platforms. Vertically-spaced antenna beams are preferable to horizontally-spaced beams because the refractive index irregularities change character more rapidly with height than with horizontal position.

For real time transmission, space and/or angle diversity are beneficial for spectrum conservation, but time diversity (usually with the addition of error correcting codes) may also be of interest when real time transmission is not a requirement, and where space and spectrum considerations are important (Hall, 1979).

3.2 Intersystem Interference

Fig. 12 (Crane, 1980) shows the propagation phenomena producing interference.

Fig. 13 shows three types of signals received by tropospheric propagation [Wikerts and Nilsson] in a study in Sweden. The high level fields produced by ducting and rain scatter cause intersystem interference.

Rain scatter on a space-earth path can cause interference at a terrestrial station. Scatter from a terrestrial to a space station is also possible. The scattering can be considered to be approximately isotropic and maximum coupling will occur when the main lobes (of the space station and terrestrial station) intersect in rain. Attenuation outside the common volume will have to be taken into consideration at frequencies above about 10 GHz.

A study of transhorizon propagation carried out over a 165 km distance at 93 MHz in Nigeria showed that [Ajayi, 1982]

(a) the condition in the troposphere favouring trans-horizon propagation existed generally from about 18h00 until about 11h00 local time.

(b) median value of signal strength is lower during the rainy season than during the dry season especially during the foggy days of the harmattan period.

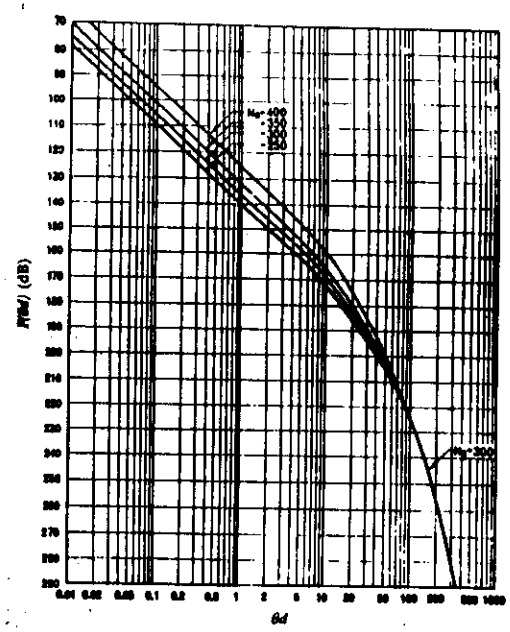

FIGURE II – *The attenuation function, F(θd), where d is in km and θ is in radians*

(CCIR, 1982)

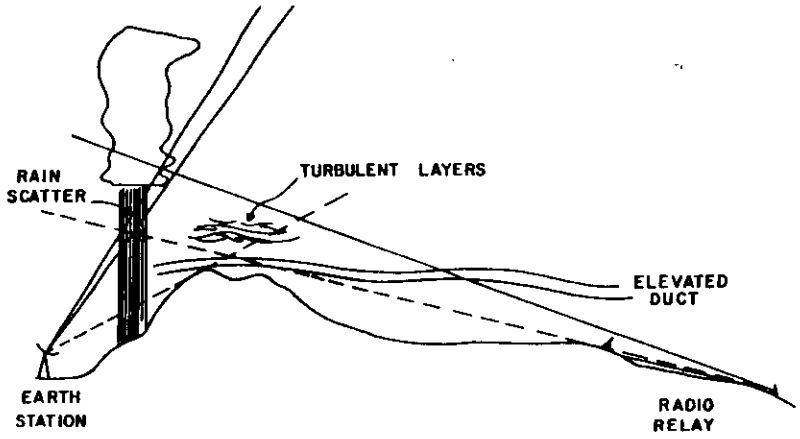

Fig. 12 PROPAGATION PHENOMENA PRODUCING INTERFERENCE [Crane, 1980]

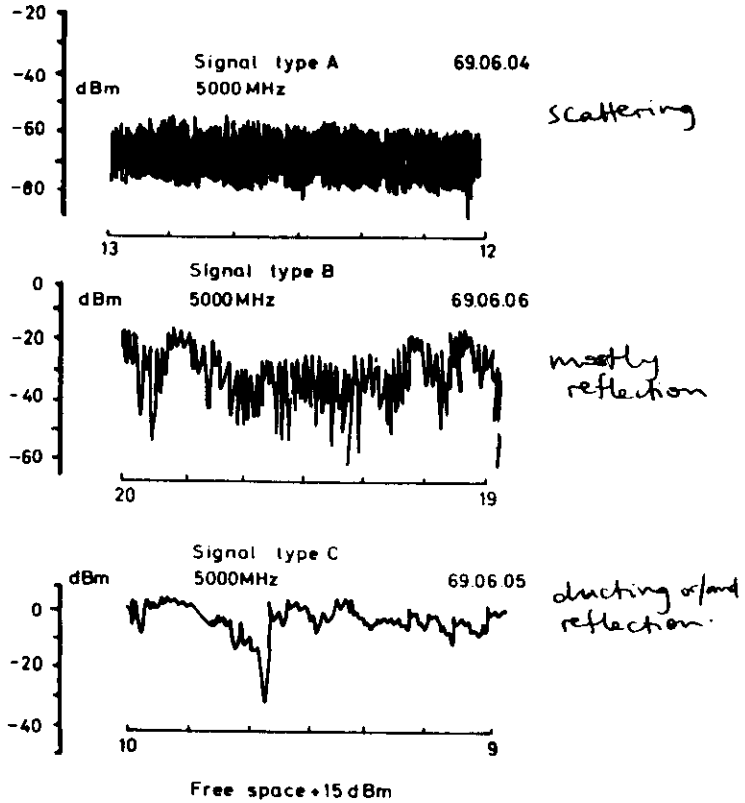

Figure 13 Signal types at 5000 MHz. (Wickerts and Nilsson)
Distance: 160 km

4. REFERENCES

1. Ajayi, G.O.: "Tranhorizon propagation and its implications to radiowave propagation at VHF and higher frequencies in Nigeria. The Nigerian Engineer, 17, 72-75, 1982.

2. Ajayi, G.O. and Odunewu, P.A.: Some characteristics of the rain height in a tropical environment. Preprint of Int. Conf. on Antennas & Propagation, Warwick, U.K. April 1989.

3. Crane, R.K.: Prediction of attenuation by rain, Environmental Research & Technology, Inc. ERT Report, 1979.

4. Crane, R.K.: A review of tranehorizon propagation phenomena. URSI Comm. F. Open Symp., Lennoxiville, Quebec, 1980.

5. Dougherty, H.T. and E.J. Dutton,: The role of elevated ducting for radio service and interference fields. U.S. Dept. of Commerce, NTIA Report-81-69, 1981

6. Lenkurt(USA): Microwave Path Engineering Considerations 6000-8000 MC, 1960

7. Lin, S.H.: Empirical calculation of microwave rain attenuation distributions on Earth-Satellite Paths, Record, EASCON '78, Arlington, Va., 372-378, 1978.

8. Manfouma, F.: Rain induced attenuation prediction model for terrestrial and satellite-Earth microwave links, Ann. des Telecomm. 42, 539-550, 1987

9. Nakagami, M.: The m-distribution – A General Formula of Intensity Distribution of Rapid fading; Contained in W.C. Hoffman (ed), "Statistical Methods in Radio Wave Propagation", Pergamon Press, pp 3-36, 1960.

10 Olsen, R.L., Martin, L. and Tjelta, T.: "A review of the role of surface reflection in multipath propagation over line-of-sight terrestrial microwave links, AGARD Conference Proc. No 407, Paris, France.

11 Rue, O.: The statistical dependence of rain height on rain rate, and its use in rain attenuation prediction. Swedish Telecom. Radio Report, R I 01/85.

12. Stephansen, E.T.: Review of clear-air propagation on line-of-sight radio paths. URSI Comm. F. Open Symp. Lennoxville, Canada, 1980.

13 Wickerts, S. and Nilsson, L.: The occurrence of very high field strengths at beyond the horizon propagation over sea in the frequency range 60 – 5000 MHz. National Defence Research Institute, Stockholm, Sweden, Research Report